Scheme for adding electron-nucleus cusps to Gaussian orbitals

A. Ma, M. D. Towler, N. D. Drummond, and R. J. Needs
Theory of Condensed Matter Group, Cavendish Laboratory,
University of Cambridge, Madingley Road, Cambridge, CB3 0HE, United Kingdom
(Dated: April 16, 2005)

A simple scheme is described for introducing the correct cusps at nuclei into orbitals obtained from Gaussian basis set electronic structure calculations. The scheme is tested with all-electron variational quantum Monte Carlo (VMC) and diffusion quantum Monte Carlo (DMC) methods for the Ne atom, the H_2 molecule, and fifty-five molecules from a standard benchmark set. It greatly reduces the variance of the local energy in all cases and slightly improves the variational energy. One therefore expects the scheme to yield a general improvement in the efficiency of all-electron VMC and DMC calculations using Gaussian basis sets.

PACS numbers: 71.10.-w, 31.25.Eb

I. INTRODUCTION

Quantum Monte Carlo (QMC) methods provide a very promising approach for calculating accurate energies of many-electron systems. For low atomic number (Z) atoms it is quite common to use all-electron QMC techniques where every electron is explicitly included in the simulation, but the computational cost rises rapidly with Z. The scaling behavior can be considerably improved by replacing the core electrons with pseudopotentials, but this procedure inevitably introduces errors and it is clearly desirable to perform highly accurate all-electron QMC calculations for a wider range of atomic numbers than has been attempted before. In this article we demonstrate that an accurate representation of the electron–nucleus cusps[1] in the wave function is, not unexpectedly, of critical importance in such calculations.

The VMC technique and the more accurate DMC technique[2] require an approximate many-body trial wave function, which is normally written as the product of a Slater determinant, or sum of determinants, and a Jastrow correlation factor. The quality of the Slater part of the wave function is extremely important. For small molecules the orbitals are usually obtained from a single-particle method such as Hartree-Fock (HF) theory or density-functional theory, or sometimes from a multi-determinant description such as the Multi-Configuration Self-Consistent Field (MCSCF) method. Such calculations are normally performed using standard quantum chemistry packages which use an atom-centered Gaussian basis.

One of the problems with Gaussian basis sets is that they are unable to describe the cusps in the single-particle orbitals at the nuclei that would be present in the exact HF orbitals, because the Gaussian basis functions have zero gradient at the nuclei on which they are centered. This can lead to considerable difficulties in QMC simulations. In both VMC and DMC methods the energy is calculated as the average over many points in the electron configuration space of the local energy, $E_L = \Psi^{-1}\hat{H}\Psi$, where $\hat{H}$ is the Hamiltonian and Ψ is the many-electron trial wave function. When an electron approaches a nucleus of charge Z the potential energy contribution to E_L diverges as $-Z/r$, where r is the distance from the nucleus.[3] The kinetic energy operator acting on the cusps in the wave function must therefore supply an equal and opposite divergence in the local kinetic energy, because the local energy is constant everywhere in the configuration space if Ψ is an eigenstate of the Hamiltonian. Unfortunately, when using orbitals expanded in a Gaussian basis set, the kinetic energy is finite at the nucleus and therefore E_L diverges. In practice one finds that the local energy has wild oscillations close to the nucleus, which give rise to a large variance in the energy. This is undesirable in VMC, but within DMC it can lead to severe bias and even to catastrophic numerical instabilities.

Within a basis of Slater-type orbitals (STOs) it is possible to enforce the cusp conditions by imposing constraints on the solutions of the self-consistent equations[4]. In principle this appears to be an excellent solution to the cusp problem, but STO codes will have to be developed much further for this to become a practical approach for the range of problems we study. We are interested in molecular systems, for which we require both single- and multi-determinant wave functions, and extended systems modeled within periodic boundary conditions. We are not aware of STO codes which are suitable for all of these purposes and, besides, the modifications to an STO code required to impose the cusp conditions are non-trivial.

It is not in general possible to satisfy the cusp conditions using STOs in which each basis function is chosen to obey the cusp conditions at the nucleus on which it is centered, because of the contributions from the tails of STOs centered on other nuclei. Manten and Lüchow[5] have developed a scheme for applying cusp corrections to Gaussian orbitals in QMC calculations but, as it similarly relies on correcting individual atom-centered basis functions, it is not a full solution to the cusp problem.

An alternative solution to the cusp problem might be to enforce the electron–nucleus cusp condition using the Jastrow factor. This is feasible and we have implemented it, but we found it to be unsatisfactory because a very large number of variable parameters are required to obtain a good trial wave function.[6]

The solution we have adopted in our computer code CASINO[7] involves the direct modification of the molecular orbitals so that each of them obeys the cusp condition at each nucleus. This ensures that the local energy remains finite whenever an electron is in the vicinity of a nucleus, although it generally has a discontinuity at the nucleus. We apply this modification to the molecular orbitals, and no alterations to the Gaussian basis set codes are required. We note that our algorithm could also be used for orbitals expanded in other atom-centered basis sets, such as STOs, again without the need to modify the code which generated them.

II. ELECTRON–NUCLEUS CUSP CORRECTIONS

The Kato cusp condition[1] applied to an electron at $\mathbf{r}_i$ and a nucleus of charge Z at the origin is

$$\left(\frac{\partial\langle\Psi\rangle}{\partial r_i}\right)_{r_i=0} = -Z\langle\Psi\rangle_{r_i=0} \,, \tag{1}$$

where $\langle\Psi\rangle$ is the spherical average of the many-body wave function about $\mathbf{r}_i = 0$. For a determinant of orbitals to obey the Kato cusp condition at the nuclei it is sufficient for every orbital to obey Eq. (1) at every nucleus. We need only correct the orbitals which are non-zero at a particular nucleus because the others already obey Eq. (1). This is sufficient to guarantee that the local energy is finite at the nucleus provided at least one orbital is non-zero there. In the unlikely case that all of the orbitals are zero at the nucleus then the probability of an electron being at the nucleus is zero and it is not important whether Ψ obeys the cusp condition.

An orbital, ψ, expanded in a Gaussian basis set can be written as

$$\psi = \phi + \eta \,, \tag{2}$$

where ϕ is the part of the orbital arising from the s-type Gaussian functions centered on the nucleus in question (which, for convenience is at $\mathbf{r} = 0$), and η is the rest of the orbital. The spherical average of ψ about $\mathbf{r} = 0$ is given by

$$\langle\psi\rangle = \phi + \langle\eta\rangle \,. \tag{3}$$

In our scheme we seek a corrected orbital, $\tilde{\psi}$, which differs from ψ only in the part arising from the s-type Gaussian functions centered on the nucleus, i.e.,

$$\tilde{\psi} = \tilde{\phi} + \eta \,. \tag{4}$$

The correction, $\tilde{\psi} - \psi$, is therefore spherically symmetric about the nucleus. We now demand that $\tilde{\psi}$ obeys the cusp condition at $\mathbf{r} = 0$,

$$\left(\frac{d\langle\tilde{\psi}\rangle}{dr}\right)_0 = -Z\langle\tilde{\psi}\rangle_0 \,. \tag{5}$$

Note that $\langle\eta\rangle$ is cusp-less because it arises from the Gaussian basis functions centered on the origin with non-zero angular momentum, whose spherical averages are zero, and the tails of the Gaussian basis functions centered on other sites, which must be cusp-less at the nucleus in question. We therefore obtain

$$\left(\frac{d\tilde{\phi}}{dr}\right)_0 = -Z\left(\tilde{\phi}(0) + \eta(0)\right) \,. \tag{6}$$

We use Eq. (6) as the basis of our scheme for constructing cusp-corrected orbitals.

III. CUSP CORRECTION ALGORITHM

One could conceive of correcting the orbitals either by adding a function to the Gaussian orbital inside some reasonably small radius, multiplying by a function (e.g., using the Jastrow factor as mentioned in Sec. I), or by replacing the orbital near the nucleus by a function which obeys the cusp condition. However, as the local energy obtained from Gaussian orbitals shows wild oscillations close to the nucleus, the best option seems to be the latter one: replacement of the orbital inside some small radius by a well-behaved form.

We apply a cusp correction to each orbital at each nucleus at which it is non-zero. Inside some cusp correction radius r_c we replace ϕ, the part of the orbital arising from s-type Gaussian functions centered on the nucleus in question, by

$$\tilde{\phi} = C + \mathrm{sgn}[\tilde{\phi}(0)]\exp[p(r)] = C + R(r). \tag{7}$$

In this expression $\mathrm{sgn}[\tilde{\phi}(0)]$ is ± 1, reflecting the sign of $\tilde{\phi}$ at the nucleus, and C is a shift chosen so that $\tilde{\phi} - C$ is of one sign within r_c. This shift is necessary since the uncorrected s-part of the orbital ϕ may have a node where it changes sign inside the cusp correction radius, and we wish to replace ϕ by an exponential function, which is necessarily of one sign everywhere. The polynomial p is given by

$$p = \alpha_0 + \alpha_1 r + \alpha_2 r^2 + \alpha_3 r^3 + \alpha_4 r^4 \,, \tag{8}$$

and we determine α_0, α_1, α_2, α_3, and α_4 by imposing five constraints on $\tilde{\phi}$. We demand that the value and the first and second derivatives of $\tilde{\phi}$ match those of the s-part of the Gaussian orbital at $r = r_c$. We also require that the cusp condition is satisfied at $r = 0$. We use the final degree of freedom to optimize the behavior of the local energy in a manner to be described below. However, if we impose such a constraint directly the equations satisfied by the α_i cannot be solved analytically. This is inconvenient and we found that a superior algorithm was obtained by imposing a fifth constraint which allows the equations to be solved analytically, and then searching over the value of the fifth constraint for a "good solution". To this end we chose to constrain the value of $\tilde{\phi}(0)$. With these constraints we have:

1.

$$\ln|\tilde{\phi}(r_c) - C| = p(r_c) = X_1; \tag{9}$$

2.

$$\frac{1}{R(r_c)}\frac{d\tilde{\phi}}{dr}\bigg|_{r_c} = p'(r_c) = X_2; \tag{10}$$

3.

$$\frac{1}{R(r_c)}\frac{d^2\tilde{\phi}}{dr^2}\bigg|_{r_c} = p''(r_c) + p'^2(r_c) = X_3; \tag{11}$$

4.

$$\frac{1}{R(0)}\frac{d\tilde{\phi}}{dr}\bigg|_{0} = p'(0) = -Z\left(\frac{C + R(0) + \eta(0)}{R(0)}\right) = X_4; \tag{12}$$

5.

$$\ln|\tilde{\phi}(0) - C| = p(0) = X_5. \tag{13}$$

Although the constraint equations are non-linear, they can be solved analytically, giving

$$\begin{aligned}
\alpha_0 &= X_5 \\
\alpha_1 &= X_4 \\
\alpha_2 &= 6\frac{X_1}{r_c^2} - 3\frac{X_2}{r_c} + \frac{X_3}{2} - 3\frac{X_4}{r_c} - 6\frac{X_5}{r_c^2} - \frac{X_2^2}{2} \\
\alpha_3 &= -8\frac{X_1}{r_c^3} + 5\frac{X_2}{r_c^2} - \frac{X_3}{r_c} + 3\frac{X_4}{r_c^2} + 8\frac{X_5}{r_c^3} + \frac{X_2^2}{r_c} \\
\alpha_4 &= 3\frac{X_1}{r_c^4} - 2\frac{X_2}{r_c^3} + \frac{X_3}{2r_c^2} - \frac{X_4}{r_c^3} - 3\frac{X_5}{r_c^4} - \frac{X_2^2}{2r_c^2}.
\end{aligned} \tag{14}$$

Our procedure is to solve Eq. (14) using an initial value of $\tilde{\phi}(0) = \phi(0)$. We then vary $\tilde{\phi}(0)$ so that the "effective one-electron local energy",

$$\begin{aligned}
E_L^s(r) &= \tilde{\phi}^{-1}\left[-\frac{1}{2}\nabla^2 - \frac{Z_{\text{eff}}}{r}\right]\tilde{\phi} \qquad (15)\\
&= -\frac{1}{2}\frac{R(r)}{C + R(r)}\left[\frac{2p'(r)}{r} + p''(r) + p'^2(r)\right] - \frac{Z_{\text{eff}}}{r},
\end{aligned}$$

is well-behaved. Here the effective nuclear charge Z_{eff} is given by

$$Z_{\text{eff}} = Z\left(1 + \frac{\eta(0)}{C + R(0)}\right), \tag{16}$$

which ensures that $E_L^s(0)$ is finite when the cusp condition of Eq. (12) is satisfied.

We studied the effective one-electron local energies obtained using Eq. (15) with $Z_{\text{eff}} = Z$ for the $1s$ and $2s$ all-electron Hartree-Fock orbitals of neutral atoms calculated by numerical integration on fine radial grids for atoms up to $Z = 82$. We noticed that the quantity $E_L^s(r)/Z^2$ is only weakly dependent on Z in the range $r < 1.5/Z$. We therefore chose an "ideal" effective one-electron local energy curve given by

$$\begin{aligned}
\frac{E_L^{\text{ideal}}(r)}{Z^2} &= \beta_0 + \beta_1 r^2 + \beta_2 r^3 + \beta_3 r^4 \\
&\quad + \beta_4 r^5 + \beta_5 r^6 + \beta_6 6r^7 + \beta_7 r^8.
\end{aligned} \tag{17}$$

The values chosen for the coefficients were $\beta_1 = 3.25819$, $\beta_2 = -15.0126$, $\beta_3 = 33.7308$, $\beta_4 = -42.8705$, $\beta_5 = 31.2276$, $\beta_6 = -12.1316$, $\beta_7 = 1.94692$, obtained by fitting to the data for the $1s$ orbital of the carbon atom. The value of β_0 depends on the particular atom and its environment. The ideal effective one-electron local energy for a particular orbital is chosen to have the functional form of $E_L^{\text{ideal}}(r)$, but with the constant value β_0 chosen so that the effective one-electron local energy is continuous at r_c. Hydrogen is treated as a special case as the $1s$ orbital of the isolated atom is only half-filled, and we use $E_L^{\text{ideal}}(r) = \beta_0$.

We wish to choose $\tilde{\phi}(0)$ so that $E_L^s(r)$ is as close as possible to $E_L^{\text{ideal}}(r)$ for $0 < r < r_c$, i.e., the effective one-electron local energy is required to follow the "ideal" curve as closely as possible. In our current implementation we find the best $\tilde{\phi}(0)$ by minimizing the maximum square deviation from the ideal energy, $[E_L^s(r) - E_L^{\text{ideal}}(r)]^2$, within this range. Beginning with $\tilde{\phi}(0) = \phi(0)$, we first bracket the minimum then refine $\tilde{\phi}(0)$ using a simple golden section search. In principle we are more interested in $E_L^s(r)$ being close to $E_L^{\text{ideal}}(r)$ near r_c than near zero because the probability of an electron being near r_c is normally much greater than it being near the nucleus. One might therefore consider using a weighting factor and minimizing, e.g., $[r(E_L^s(r) - E_L^{\text{ideal}}(r))]^2$. In practical calculations this was found not to improve the result in general and weighting factors were not used in our final implementation.

It is clearly important to find an automatic procedure for choosing appropriate values of the cusp correction radii. Although the final quality of the wave function in QMC calculations is expected to have only a relatively weak dependence on its precise value, the optimal cusp correction radius r_c for each orbital and nucleus should depend on the quality of the basis set and on the shape of the orbital in question. In particular one would expect the cusp correction radii to become smaller as the quality of the basis set is improved. Although clearly many other schemes are possible, we choose the r_c in our implementation as follows. The maximum possible cusp correction radius is taken to be $r_{c,max} = 1/Z$. The actual value of r_c is then determined by a universal parameter c_c for which a default value of 50 was found to be reasonable. The cusp correction radius r_c for each orbital and nucleus is set equal to the largest radius less than $r_{c,max}$ at which the deviation of the effective one-electron local energy calculated with ϕ from the ideal curve has a magnitude greater than Z^2/c_c. Appropriate polynomial coefficients α_i and the resulting maximum deviation of the

effective one-electron local energy from the ideal curve are then calculated for this r_c. As a final refinement one might then allow the code to vary r_c over a relatively small range centered on the initial value, recomputing the optimal polynomial cusp correction at each radius, in order to optimize further the behavior of the effective one-electron local energy. This is done by default in our implementation.

When a Gaussian orbital can be readily identified as, for example, a $1s$ orbital, it generally does not have a node within $r_{c,max}$. In many cases, however, some of the molecular orbitals have small s-components which may have nodes close to the nucleus. The possible presence of nodes inside the cusp correction radius complicates the procedure because the effective one-electron local energy diverges there. One could simply force the cusp correction radius to be less than the radius of the node closest to the nucleus, but in practice nodes can be very close to the nucleus and such a constraint severely restricts the flexibility of the algorithm. In practice we define small regions around each node where the effective one-electron local energies are not taken into account during the minimization, and from which the cusp correction radius is excluded.

IV. RESULTS

The above procedure has been implemented in the CASINO[7] code for both finite systems and systems periodic in one, two and three dimensions where the orbitals are represented in Gaussian basis sets. The code is capable of using other kinds of basis set including plane waves and a local spline re-expansion of plane wave orbitals[8], but in such cases one uses pseudopotentials. Generally these can be forced to be finite at the nucleus[9] and therefore do not lead to cusps in the orbitals. Some pseudopotentials however, such as those of the Stuttgart group[10], diverge like $-1/r$ at the nucleus. As calculations with these pseudopotentials are normally performed with Gaussian basis sets, our cusp correction scheme could in principle be employed to improve the behavior of the local energy in QMC applications that use them.

In terms of performance, one finds in practice that the set-up procedure for calculating the optimum cusp parameters before the main QMC calculation starts takes a negligible amount of CPU time – at most a few seconds for large systems. For atoms and molecules the main orbital evaluation routine is slowed by a few per cent when calculating the cusp corrections. This increases to around ten per cent in the periodic case, which is acceptable given the improved stability and the reduction in the variance of the local energy obtained in all-electron calculations.

To illustrate the improved capabilities of the code, we have performed test calculations on the Ne atom, the H_2 molecule, and fifty-five molecules of a standard test set, which will now be described.

A. The Ne atom

In Fig. 1 we plot the $1s$ orbital of the Ne atom with and without the cusp correction. The HF calculations were performed using the CRYSTAL code[11] with a reasonably good Gaussian basis set composed of 1 contracted s Gaussian of 6 primitives, 6 uncontracted s functions, and 6 uncontracted p functions, the exponents and contraction coefficients of which were optimized to minimize the energy. This basis gives a ground state HF energy of -128.538450 a.u., which is only slightly higher than the exact HF energy of -128.547098 a.u.

The $1s$ cusp correction radius calculated using the scheme outlined above is $r_c = 0.0875$ a.u. This is a little less than the size of the Bohr radius for the $1s$ orbital of Ne ($1/Z = 0.1$ a.u.), but the constraints at $r = r_c$ and $r = 0$ ensure that the corrected orbital does not deviate much from the original Gaussian orbital except close to $r = 0$. The inset in Fig. 1 shows the behavior near the nucleus; the cusp in the corrected orbital is readily apparent.

The effective one-electron local energy of Eq. (15) is plotted as a function of distance from the nucleus in Fig. 2 for the uncorrected Gaussian orbital, the cusp-corrected orbital, and for a quasi-exact numerical HF orbital. The effective one-electron local energy for the exact HF orbital remains well-behaved over the entire range. The effective one-electron local energy for the uncorrected Gaussian orbital oscillates far from the nucleus, and the magnitude of the oscillations grows rapidly at small r, where it reaches a maximum positive value of about 280 a.u., and then tends to $-\infty$ at $r = 0$. The effective one-electron local energy from the cusp-corrected orbital follows the uncorrected one from large r down to $r = r_c$, where its gradient changes abruptly and it begins to approximate the form for the exact orbital rather closely.

We tested the cusp-corrected wave functions within VMC and DMC calculations using the CASINO code.[7] First we performed VMC calculations for Ne with Slater-Jastrow wave functions including the cusp-corrected orbitals for different values of r_c. The Jastrow factor[6] contained forty-four variable parameters, whose optimal values were determined separately at each value of r_c by minimizing the variance of the energy.[12,13] In Fig. 3 we plot the VMC energy including statistical error bars versus the cusp correction radius of the $1s$ orbital. For $r_c = 0$ (equivalent to no cusp correction) the error bar is very large. As the cusp correction radius is increased it is apparent that the error bar on the energy is greatly reduced, and that the variational energy itself is slightly lowered for $r_c < 0.12$ a.u. For $r_c > 0.12$ a.u. the VMC energy begins to increase, although the variance is still quite small. These results indicate that the absence of the cusps in orbitals expanded in Gaussian basis sets is the largest source of variance in the energy, and that the cusp correction has removed this source of variance and has improved the overall quality of the wave function.

We also note that the results are not very sensitive to r_c, with values between 0.05 a.u. and 0.1 a.u. giving almost the same results. This is important because it suggests that schemes for choosing r_c automatically, such as the one presented in Sec. III, can be successful.

In Fig. 4 we show the local energy of Ne, calculated with the full many-body Hamiltonian, as a function of the separation of an electron from the nucleus. This plot was generated by taking an electron configuration from a VMC run and then calculating the local energy as the electron closest to the nucleus was moved in a straight line through the nucleus. When the cusp correction is included the local energy is seen to be finite at the origin (but with a finite discontinuity whose magnitude depends on the positions of all the electrons). The local energy for the cusp-corrected wave function never strays very far from the value which it would have for the exact wave function. When the cusp correction is not imposed the local energy shows wild oscillations of similar magnitude to those of the effective one-electron local energy in Fig. 2.

We also tested the cusp-corrected wave function in DMC calculations and we obtained a DMC energy (extrapolated to zero time step) of $-128.9218(2)$ a.u. This energy is significantly higher than the exact (non-relativistic and infinite-nuclear-mass) energy of -128.9376 a.u.[14,15] due to the use of the fixed-node approximation, but it is close to the value of $-128.9238(7)$ a.u. that we obtained within DMC using quasi-exact numerical HF orbitals.[6]

In order to investigate the range of atomic numbers for which converged all-electron DMC calculations can feasibly be performed, we have also calculated the total energies of the noble gas atoms Ar, Kr and Xe ($Z = 18$, 36, 54). Details of these calculations, together with an analysis of the practical scaling behavior of the CPU time with Z, will be given in a separate publication.[16]

B. The H_2 molecule

We have also tested our scheme for small molecules, in which the contributions from the tails of the Gaussians centered on other sites described by the η term in Eq. (6) are significant. As a test case we studied the H_2 molecule, with a bond length of 0.7395 Å. We used an uncontracted Gaussian basis set consisting of 11 s functions and a single p polarization function, with all exponents optimized to minimize the energy. The final HF energy obtained was -1.128852 a.u. In Fig. 5 we plot the local energy of the H_2 molecule calculated with the many-body Hamiltonian as one of the electrons is moved through a nucleus. Without the cusp correction the local energy oscillates and diverges at the nucleus, but when the full cusp correction is added the local energy is well behaved. To understand the importance of including contributions from the tails of Gaussians centered on other sites we have also plotted results with $\eta(0)$ in Eq. (6) artificially set to zero, meaning that such contributions are not taken into account. (In fact, $\eta(0) = 0.1879$ out of a total $\phi(0) = 0.9650$.) It is apparent from the figure that although the local energy does not oscillate, it still diverges at the nucleus, demonstrating that one cannot satisfy the cusp conditions exactly without taking into account basis function contributions from other nuclei. This example demonstrates that our cusp correction scheme completely removes the divergence in the local energy when an electron moves through a nucleus, even in the polyatomic case.

C. Standard test set of small molecules

In order to demonstrate that our cusp-correction scheme gives a general improvement across a wide range of chemical environments we have performed VMC calculations with single-determinant wave functions without a Jastrow factor (HFVMC calculations) for fifty-five molecules taken from a standard benchmark set. Thirty-one of these molecules were originally used to fit the semi-empirical G1 theory[17] with a further twenty-four molecules containing elements from the second row of the periodic table added to the set later[18]. We used the standard molecular geometries specified for use with this set, which were originally optimized at the MP2/6-31G(d) level. We emphasize that we used the automatic version of our algorithm with $c_c = 50$, and further optimization of the cusp correction radius was not attempted.

In Table I we give results for the molecular HF energies, $E_{\rm HF}$, calculated using the CRYSTAL code and for the HFVMC energies, $E_{\rm HFVMC}$, (obtained with and without cusp corrections) from the CASINO code. The HFVMC energies were calculated from 250,000 samples in the electron configuration space. The statistical error bars on the mean energies are given by the number in brackets which represents the standard error in the last digit. The table also shows the variance of the local energy, σ^2, for each molecule, again with and without cusp corrections. The error bars on the values of σ^2 obtained without cusp corrections are very large, and the figure in brackets represents the approximate standard error in the whole number.

It is clear that there is a general and very significant reduction in the variance in the local energy for all fifty-five molecules on introducing the cusp correction, with a consequent reduction in the standard error in the mean energies by approximately an order of magnitude. This is also apparent in Fig. 6 where the local energy is plotted as a function of move number for the CH_3Cl molecule. In the absence of the cusp correction there are a great many large spikes in the VMC energy resulting from the divergences in the local energy near the nucleus. These are significantly reduced when the orbitals are corrected. We also found that the correlation length for the energy was considerably reduced by incorporating the cusp corrections.

In order to gauge the accuracy of all-electron quantum Monte Carlo and of our cusp-correction scheme, we have performed benchmark calculations of the DMC energies of this set of molecules and their constituent atoms, and hence the molecular atomization energies and their mean absolute deviation from experiment. Details of these calculations will appear in a separate publication[19], together with a comparison with the results of Grossman[20] who performed similar DMC calculations using pseudopotentials.

V. CONCLUSIONS

We have described and tested a simple, automatic, numerically-stable scheme for introducing the correct cusp at the nucleus into orbitals obtained from calculations using Gaussian basis sets. This ensures that the local energy is finite when an electron and nucleus are coincident. Our scheme may readily be adapted for use with other atom-centered basis sets.

The scheme has been devised for use within all-electron VMC and DMC calculations. We have performed extensive tests for the Ne atom, the H_2 molecule and a fifty-five molecule benchmark set. In all cases it greatly reduces the variance of the energy and also slightly reduces the variational energy. This technical development should lead to improved results from all-electron VMC and DMC calculations.

VI. ACKNOWLEDGMENTS

We acknowledge financial support from the Engineering and Physical Sciences Research Council (EPSRC) of the United Kingdom.

[1] T. Kato, Commun. Pure Appl. Math. **10**, 151 (1957).
[2] W. M. C. Foulkes, L. Mitas, R. J. Needs, and G. Rajagopal, Rev. Mod. Phys. **73**, 33 (2001).
[3] We use Hartree atomic units, $\hbar = |e| = m_e = 4\pi\epsilon_0 = 1$, throughout this article.
[4] P. T. A. Galek, N. C. Handy, A. J. Cohen, G. K.-L. Chan, Chem. Phys. Lett. **404**, 156 (2005).
[5] S. Manten and A. Lüchow, J. Chem. Phys. **115**, 5362 (2001).
[6] N. D. Drummond, M. D. Towler, and R. J. Needs, Phys. Rev. B **70**, 235119 (2004).
[7] R. J. Needs, M. D. Towler, N. D. Drummond, and P. R. C. Kent, CASINO version 1.7 User Manual, University of Cambridge, Cambridge (2004).
[8] D. Alfè and M. J. Gillan, Phys. Rev. B **70**, 161101(R) (2004).
[9] J. R. Trail and R. J. Needs, J. Chem. Phys. **122**, 014112 (2005); *ibid.* unpublished.
[10] G. Igel-Mann, H. Stoll, and H. Preuss, Mol. Phys. **65**, 1321 (1988).
[11] V. R. Saunders, R. Dovesi, C. Roetti, M. Causà, N. M. Harrison, R. Orlando, and C. M. Zicovich-Wilson, CRYSTAL98 *User's Manual*, University of Torino, Torino (1998).
[12] C. J. Umrigar, K. G. Wilson, and J. W. Wilkins, Phys. Rev. Lett. **60**, 1719 (1988).
[13] P. R. C. Kent, R. J. Needs, and G. Rajagopal, Phys. Rev. B **59**, 12344 (1999).
[14] E. R. Davidson, S. A. Hagstrom, S. J. Chakravorty, V. M. Umar, and C. F. Fischer, Phys. Rev. A **44**, 7071 (1991).
[15] S. J. Chakravorty, S. R. Gwaltney, E. R. Davidson, F. A. Parpia, and C. F. Fischer, Phys. Rev. A **47**, 3649 (1993).
[16] A. Ma, M. D. Towler, N. D. Drummond, and R. J. Needs, unpublished.
[17] J. A. Pople, M. Head-Gordon, D. J. Fox, K. Raghavachari, and L. A. Curtiss, J. Chem. Phys. **90**, 5622 (1989).
[18] L. A. Curtiss, C. Jones, G. W. Trucks, K. Raghavachari, and J. A. Pople, J. Chem. Phys. **93**, 2537 (1990).
[19] M. D. Towler, unpublished.
[20] J. C. Grossman, J. Chem. Phys. **117**, 1434 (2002).

Molecule	E_{HF} (a.u.)	E_{HFVMC} (a.u.) (no cusp correction)	σ^2 (a.u.)	E_{HFVMC} (a.u.) (cusp correction)	σ^2 (a.u.)
BeH	-15.1519	-15.153(5)	19(4)	-15.1520(7)	3.04(4)
C_2H_2	-76.8435	-76.86(2)	236(64)	-76.850(2)	17.2(2)
C_2H_4	-78.0602	-78.13(3)	299(67)	-78.065(2)	17.6(2)
C_2H_6	-79.2567	-79.24(2)	156(31)	-79.259(2)	18.0(2)
CH	-38.2809	-38.31(1)	160(48)	-38.284(1)	8.2(1)
CH_2 singlet	-38.8914	-38.90(2)	252(139)	-38.891(2)	8.5(1)
CH_2 triplet	-38.9184	-38.91(1)	87(31)	-38.920(2)	8.2(1)
CH_3	-39.5761	-39.559(8)	46(9)	-39.581(2)	8.3(1)
CH_3Cl	-499.1365	-499.3(2)	13770(12046)	-499.121(9)	148(4)
CH_4	-40.2120	-40.22(2)	178(100)	-40.215(2)	8.9(1)
Cl_2	-918.9768	-919.0(1)	3850(1297)	-918.97(1)	270(2)
ClF	-558.8792	-558.72(6)	1472(218)	-558.867(9)	164(3)
ClO	-534.2931	-534.3(1)	2768(789)	-534.311(7)	150(1)
CN	-92.2325	-92.21(2)	229(45)	-92.235(2)	20.4(2)
CO	-112.7699	-112.75(2)	315(62)	-112.773(3)	27.0(4)
CO_2	-187.6880	-187.62(2)	384(39)	-187.691(3)	44.9(5)
CS	-435.3424	-435.17(5)	868(120)	-435.352(7)	121(2)
F_2	-198.7482	-198.73(3)	736(174)	-198.749(4)	51.3(8)
H_2CO	-113.9042	-114.04(8)	1541(922)	-113.909(3)	26.8(3)
H_2O	-76.0551	-76.04(2)	188(72)	-76.054(2)	18.4(3)
H_2O_2	-150.8311	-150.85(4)	800(267)	-150.835(3)	35.9(4)
H_2S	-398.7057	-398.68(6)	2355(1534)	-398.703(7)	113(1)
H_3COH	-115.0837	-115.14(4)	1113(672)	-115.088(3)	27.2(3)
H_3CSH	-437.7466	-437.81(9)	1796(678)	-437.766(8)	121(1)
HCl	-460.0976	-459.87(6)	1437(427)	-460.109(7)	135(2)
HCN	-92.9004	-92.92(2)	195(22)	-92.903(2)	21.0(3)
HCO	-113.2845	-113.28(2)	365(105)	-113.289(3)	26.7(5)
HF	-100.0541	-100.03(3)	477(200)	-100.050(3)	26.3(5)
HOCl	-534.9018	-534.86(6)	1301(141)	-534.901(8)	152(2)
Li_2	-14.8703	-14.874(3)	23(5)	-14.8711(7)	3.06(3)
LiF	-106.9778	-106.95(2)	470(199)	-106.982(3)	26.7(3)
LiH	-7.9859	-7.984(2)	6.7(9)	-7.9864(5)	1.64(3)
N_2	-108.9710	-108.96(2)	308(76)	-108.973(3)	25.1(3)
N_2H_4	-111.2203	-111.17(2)	180(22)	-111.224(3)	26.3(6)
Na_2	-323.6914	-323.67(4)	868(165)	-323.697(5)	87(2)
NaCl	-621.4350	-621.4(1)	4278(1945)	-621.425(8)	187(6)
NH	-54.9798	-54.99(3)	343(218)	-54.982(2)	12.5(5)
NH_2	-55.5849	-55.54(1)	82(21)	-55.588(2)	12.4(2)
NH_3	-56.2173	-56.17(1)	75(11)	-56.222(2)	12.7(2)
NO	-129.2943	-129.30(3)	442(91)	-129.297(3)	30.8(5)
O_2	-149.6574	-149.64(3)	520(123)	-149.663(3)	36(1)
OH	-75.4188	-75.45(2)	319(102)	-75.421(2)	18.0(3)
P_2	-681.4717	-681.42(7)	3204(1420)	-681.482(9)	195(4)
PH_2	-341.8802	-341.88(6)	1099(408)	-341.885(6)	99(3)
PH_3	-342.4814	-342.41(8)	1486(855)	-342.487(7)	97(1)
S_2	-795.0756	-795.1(1)	8525(6227)	-795.081(9)	228(3)
Si_2	-577.5901	-577.54(8)	2604(889)	-577.604(7)	157(1)
Si_2H_6	-581.3623	-581.28(5)	1135(142)	-581.377(8)	159(2)
SiH_2 singlet	-290.0261	-289.93(4)	781(191)	-290.031(6)	82(2)
SiH_2 triplet	-290.0047	-289.95(5)	1348(571)	-290.001(6)	79(1)
SiH_3	-290.6362	-290.66(6)	1352(506)	-290.629(6)	80(1)
SiH_4	-291.2569	-291.27(7)	1046(332)	-291.251(6)	82(1)
SiO	-363.8279	-363.87(8)	3688(2648)	-363.835(6)	97(1)
SO	-472.3826	-472.26(5)	1107(103)	-472.392(7)	129(1)
SO_2	-547.2624	-547.3(1)	5672(3324)	-547.286(7)	148(2)

TABLE I: HF energies and, for the VMC calculations, the variance σ^2, for the test set of fifty-five molecules.

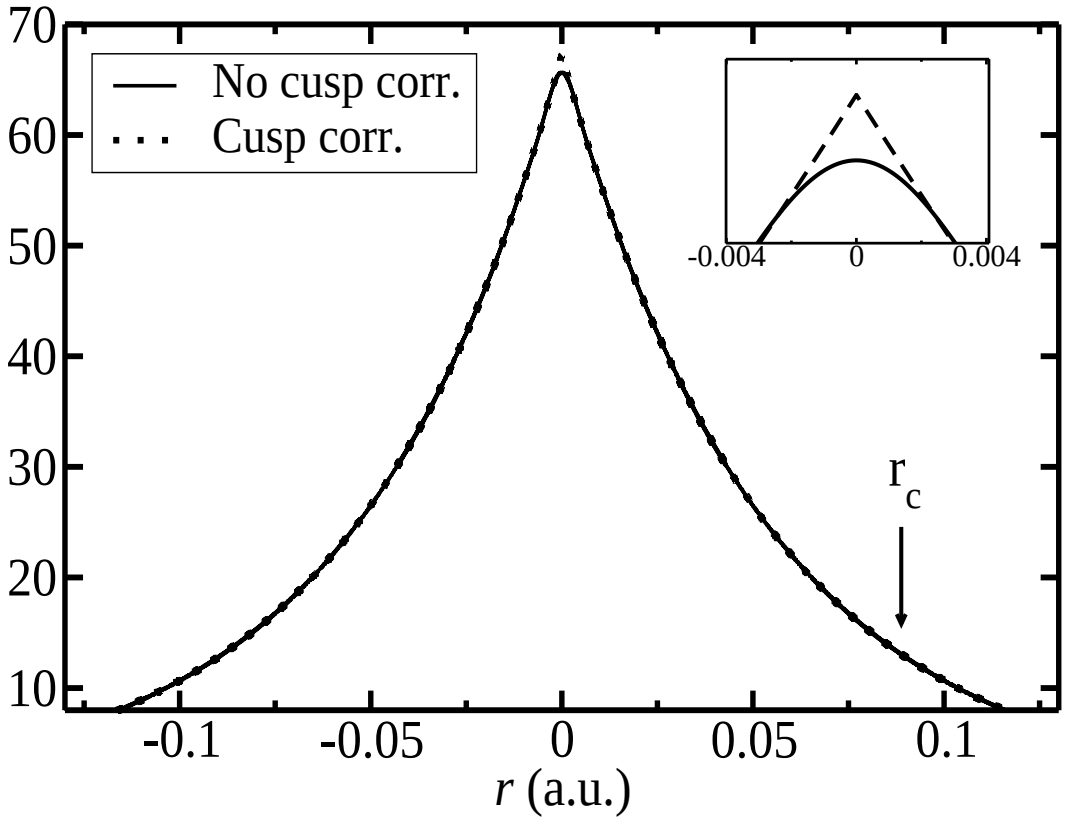

FIG. 1: The 1s orbital of the Ne atom expanded in a Gaussian basis set with and without the cusp correction.

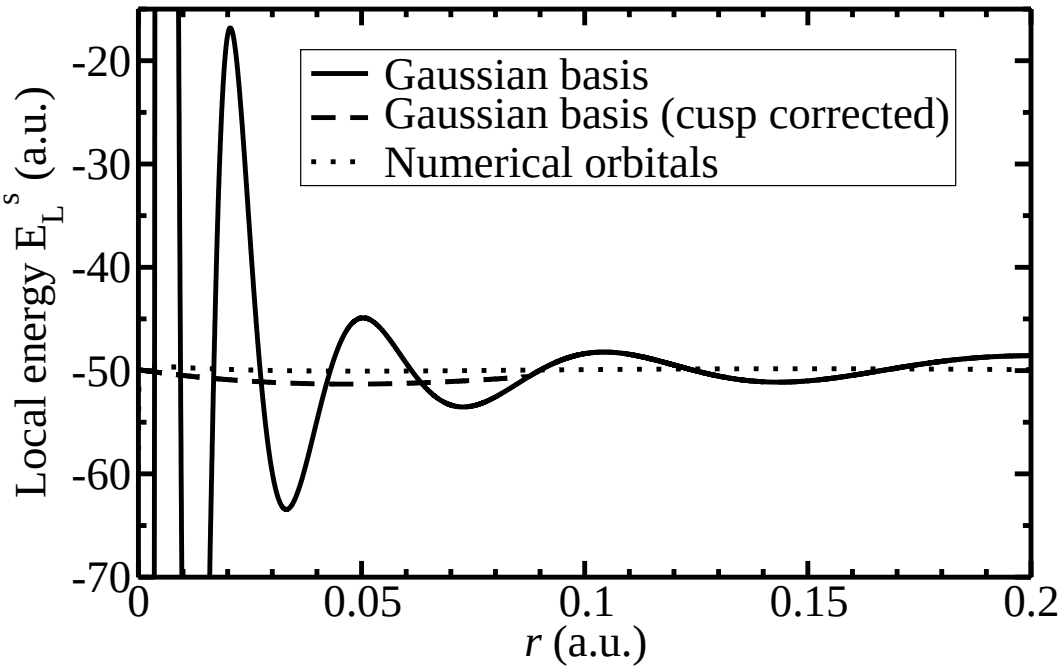

FIG. 2: The effective one-electron local energy, E_L^s, versus distance from the nucleus for the 1s orbital of Ne. Data for a quasi-exact numerical orbital, and the Gaussian orbital with and without the cusp correction.

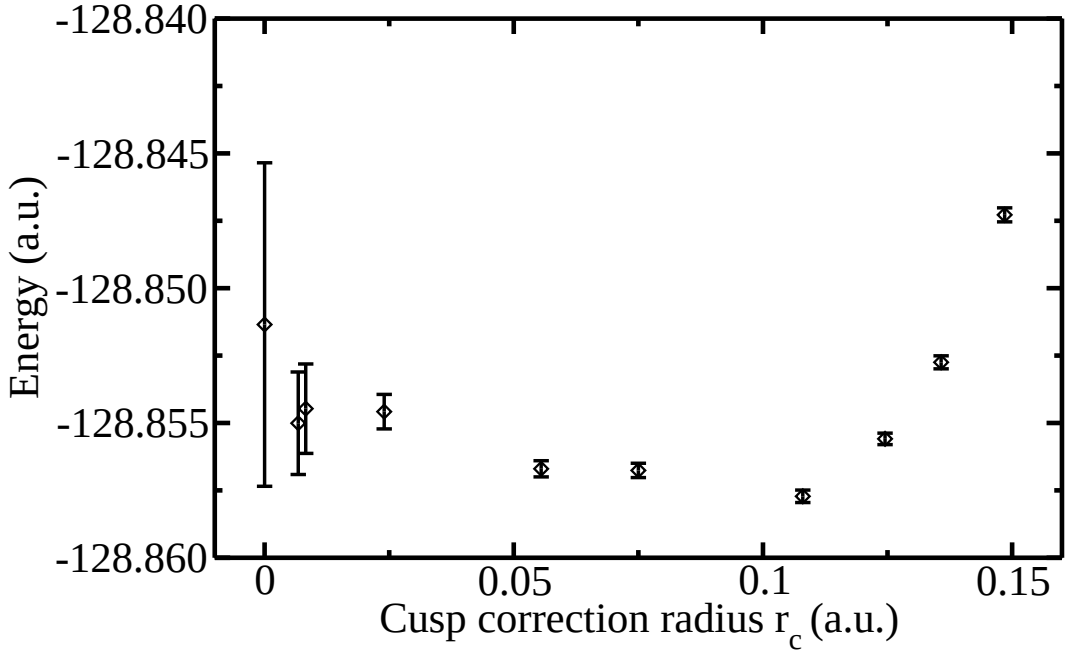

FIG. 3: The VMC energy of Ne obtained with Slater-Jastrow wave functions versus the cusp correction radius of the $1s$ orbital. The length of the error bars is twice the standard error in the mean.

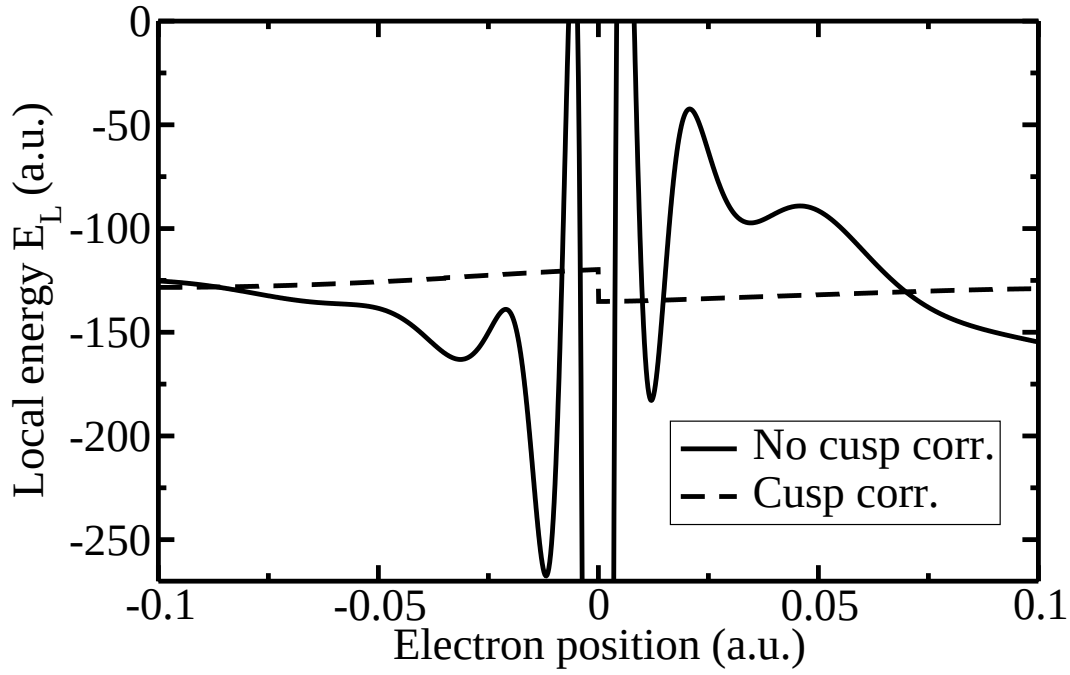

FIG. 4: The variation of the local energy, E_L, as an electron is moved through the nucleus of a Ne atom which is at the origin. Slater-Jastrow wave functions are used, both with and without the cusp correction.

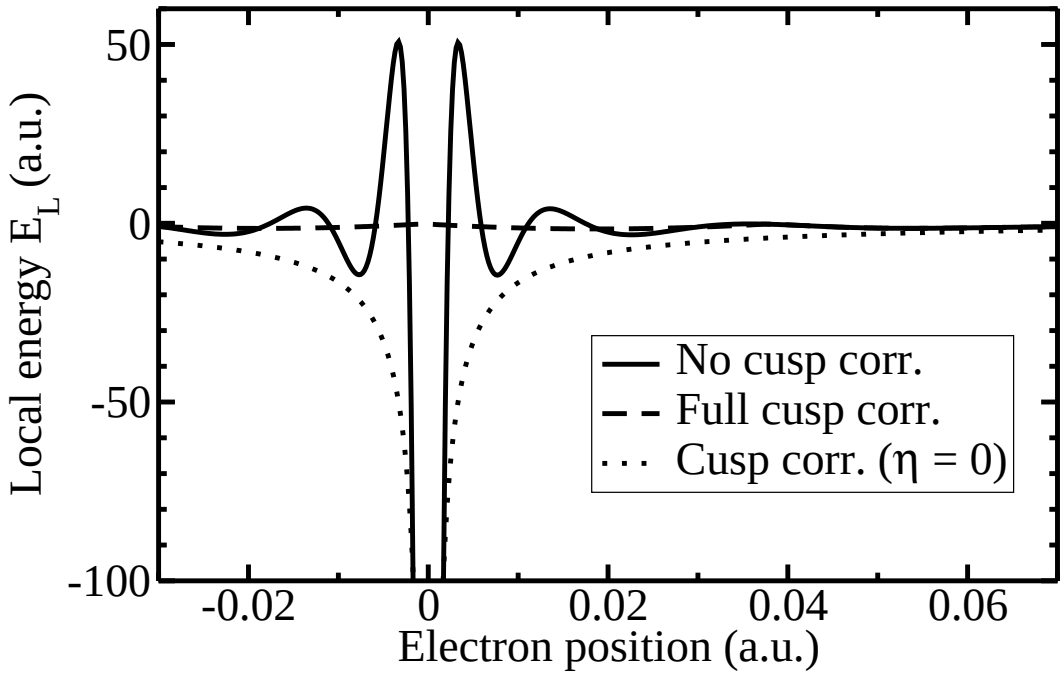

FIG. 5: The variation of the local energy, E_L, as an electron is moved through one of the nuclei of a H_2 molecule of bond length 1.4 a.u. Slater-Jastrow wave functions are used, with orbitals which are not cusp-corrected, orbitals which have the full cusp correction imposed, and orbitals which have a partial cusp correction imposed for which we set $\eta(0) = 0$.

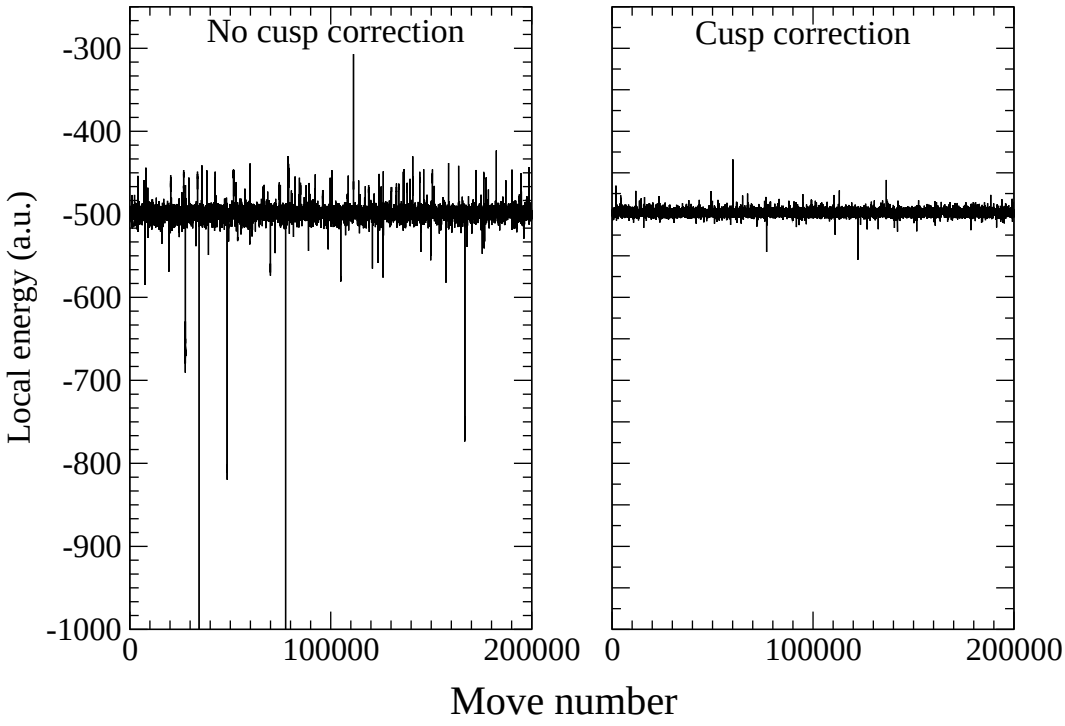

FIG. 6: Local energy after each VMC move for the CH_3Cl molecule with and without cusp corrections.